ORIGINAL ARTICLE

Determination of the influence of stent strut thickness using the finite element method: implications for vascular injury and in-stent restenosis

Houman Zahedmanesh · Caitríona Lally

Abstract Many clinical studies, including the ISAR-STEREO trial, have identified stent strut thickness as an independent predictor of in-stent restenosis where thinner struts result in lower restenosis than thicker struts. The aim of this study was to more conclusively identify the mechanical stimulus for in-stent restenosis using results from such clinical trials as the ISAR-STEREO trial. The mechanical environment in arteries stented with thin and thicker strut stents was investigated using numerical modelling techniques. Finite element models of the stents used in the ISAR-STEREO clinical trial were developed and the stents were deployed in idealised stenosed vessel geometries in order to compare the mechanical environment of the vessel for each stent. The stresses induced within the stented vessels by these stents were compared to determine the level of vascular injury caused to the artery by the stents with different strut thickness. The study found that when both stents were expanded to achieve the same initial maximum stent diameter that the thinner strut stent recoiled to a greater extent resulting in lower luminal gain but also lower stresses in the vessel wall, which is hypothesised to be responsible for the lower restenosis outcome. This study supports the hypothesis that arteries develop restenosis in response to injury, where high vessel stresses are a good measure of that injury. This study points to a critical stress level in arteries, above which an aggressive healing response leads to in-stent restenosis in stented vessels. Stents can be designed to reduce stresses in this range in arteries using preclinical tools such as numerical modelling.

1 Introduction

The majority of intrasvascular interventions cause a certain level of injury, and this injury is thought to significantly contribute to restenosis within arteries. Comparative studies have shown the benefit of coronary stenting versus balloon angioplasty alone since stenting significantly reduces elastic recoil and vascular remodelling [6]. However, excessive neointimal hyperplasia can occur post-stenting and, as a result, in-stent restenosis represents a major limitation to stenting procedures. In-stent restenosis occurs due to an adaptation of the arterial wall, whereby intima cells begin to proliferate due to the severity of the injury caused to the arterial wall, often leading to excessive neointimal hyperplasia re-stenosing the artery [7].

Two main approaches have been adopted to reduce in-stent restenosis; (1) optimising the stent design to reduce vascular injury and hence subsequent neointimal hyperplasia [17, 26], and (2) using anti-proliferative drug eluting stents to inhibit the growth of neointimal hyperplasia [8]. The delivery of an anti-proliferative drug to surrounding tissue is also significantly influenced by the stent design [11]. Clearly therefore, stent design is a key indicator of restenosis, whether bare-metal or drug-eluting.

It is therefore vital to address the issue of the mechanical stimulus for in-stent restenosis. This information would be invaluable in terms of minimising the occurrence of restenosis since it would enable stent designs to be

H. Zahedmanesh · C. Lally (✉)
School of Mechanical and Manufacturing Engineering,
Dublin City University, Glasnevin, Dublin 9, Ireland
e-mail: triona.lally@dcu.ie

optimised to lower this stimulus and also to ensure drug delivery to the areas most affected. Numerical modelling can aid in the design of cardiovascular stents and has been used extensively in recent years to offer design solutions [1, 9, 14, 15, 18].

In recent years, several clinical trials have identified stent strut thickness as an independent predictor of restenosis [2, 12, 23]. A clear conclusion from the many clinical studies on stent strut thickness is that stents with thinner struts have a lower restenosis rate, consequently, most of the current generation of stents are produced with thinner struts using high strength materials such as cobalt–chromium alloys [20].

By looking at the influence of stent strut thickness it may be possible to identify the stimulus for restenosis and more conclusively determine suitable biomechanical design criteria for stents. This may be achieved by investigating the mechanical cause of the difference in restenosis outcome for thinner and thicker strut stents using numerical modelling. The ISAR-STEREO clinical trial focussed on the influence of stent strut thickness and compared the restenosis outcome for two stents with the same design but different strut thickness [12]. In the study presented here, finite element models of these stents were developed and the stents were deployed in idealised stenosed vessels in order to compare the mechanical environment of the vessel for each stent. The stents were expanded and deployed within the arteries to scaffold open the stenosed arteries, in line with that which was carried out in the ISAR-STEREO trial. Two case studies were investigated to determine the influence of stent strut thickness on the vessel wall; (1) both stents were expanded to the same initial maximum stent diameter and (2) both stents were expanded to achieve the same final maximum stent diameter taking stent recoil into consideration. Case study 1 represents the clinical situation since stents are routinely expanded under fluoroscopy to achieve a ratio of 1.1:1 between the stent diameter and the proximal and distal diameter of the host vessel [3].

Finite element analyses were carried out to compare the stresses induced within the stented vessels by these stents, and hence to evaluate the potential of arterial injury caused by stents with different strut thickness.

2 Methods

To generate these numerical simulations, the finite element method requires a number of inputs; the geometry of the stents and the stenosed coronary arteries, the material properties of the stents and the artery, and the appropriate application of loading and boundary conditions, as described below.

2.1 Model geometry

The finite element models of the stents were generated and meshed in ANSYS (Canonsburg, PA, USA) and were generated based on the stents used in the ISAR STEREO Trial, namely the ACS RX MultiLink and the ACS MultiLink RX Duet [12]. Both stents are manufactured by the same company, namely Guidant/Advanced Cardiovascular Systems. Both stents have a similar interconnected-ring design, struts with rectangular cross-sectional areas and a width of 100 μm but different strut thickness. The strut thickness of the ACS RX MultiLink ($Mlink_{thin}$) is 50 μm and the strut thickness of the ACS MultiLink RX Duet ($Mlink_{thick}$) is 140 μm. Full three-dimensional models of the stents were developed to determine the expansion characteristics of the stents after stent deployment. The main dimensions of the stents were extrapolated from a handbook of coronary stents [25]. Both stents are available in a range of lengths, whilst the length of the stents investigated in this study was 7.2 mm. For this length, the MultiLink stents consist of six rings in the longitudinal direction with six crowns in each ring.

For both stent models, all of the parameters, such as the length and width were kept constant and the only variation between the two designs was the thickness of the struts. Both stents were simulated with an inner radius of 0.72 mm, with a corresponding outer radius of 0.77 mm for the $Mlink_{thin}$ and 0.86 mm for the $Mlink_{thick}$.

The stents are not symmetrical in the longitudinal direction, however, symmetry is observed in the circumferential direction. Due to the circumferential symmetry, only one-third was modelled in the circumferential direction with the full length in the longitudinal direction. The stent geometry was initially modelled in three-dimensional Cartesian coordinate system, representing the stent in an opened-out, planar configuration. The volumes of $Mlink_{thin}$ and $Mlink_{thick}$ were discretised by means of eight-noded isoparametric, three-dimensional brick elements. The models of $Mlink_{thin}$ and $Mlink_{thick}$ were meshed with two and three elements through the thickness respectively, see Fig. 1. These mesh densities were chosen based on mesh density studies and all elements were checked to ensure that no distorted elements were generated. The stent mesh comprised a total number of 7,794 elements for $Mlink_{thick}$ and 4,592 elements for $Mlink_{thin}$. The nodal coordinates of the meshed model were transferred from a Cartesian coordinate system into a cylindrical coordinate system, using a procedure previously reported [14] whereby the planar configuration was wrapped to represent the cylindrical structure of the stents.

The finite element software used to solve the models was ABAQUS (Pawtucket, RI, USA). ABAQUS explicit was utilised for its robust general contact algorithm and stability

Fig. 1 Finite element models of the atherosclerotic coronary arteries with crimped **a** multilink thin and **b** multilink thick stents

which enables modelling of very soft hyperelastic materials. The general contact algorithm in ABAQUS explicit with no friction between the contacting bodies was used for the analysis which enforces contact constraints using a penalty contact method. The default parameters were used to define the contact between the artery and the stent.

Each simulation model composed two bodies, the stent and the stenotic coronary artery. The thickness of atherosclerotic human coronary arteries range from 0.56 to 1.25 mm, depending upon the location of the arteries on the surface of the heart [28]. For this reason, a thickness of 0.8 mm was chosen to represent the stenosed coronary artery with the atherosclerotic localised plaque. The stenotic coronary artery was modelled as a straight 0.5-mm thick vessel with a localised plaque 0.3 mm thick and an internal radius of 1.3 mm, see Fig. 1. Eight node linear brick, reduced integration elements with hourglass control (ABAQUS element type C3D8R) were used to mesh the atherosclerotic coronary artery. Six elements were assigned through the thickness of the arterial wall. The vessel was divided into three layers; intima, media, and adventitia. The thickness of each arterial layer was discretised by two elements and each layer was of equal thickness. This closely complied with the ratio of the thickness of adventitia, media, and intima which have been reported as 0.40 ± 0.03, 0.36 ± 0.03, and 0.27 ± 0.02, respectively in [10]. Six elements were assigned through the plaque thickness in the central region. The atherosclerotic artery was meshed by a total of 121,440 elements and 135,969 nodes, see Fig. 1.

2.2 Material properties

Layer specific human coronary arterial wall properties were assigned to the artery, consisting of the intima, media and adventitia based on the data from Holzapfel et al. [10]. Human cellular atherosclerotic intimal plaque properties were assigned to the localised plaque based on the available published data from Loree et al. [16]. The material of the intima, media and adventitia were defined using third order Ogden hyperelastic constitutive equations and that of the plaque using a first order Ogden equation [22] represented by:

$$\psi = \sum_{i=1}^{N} \frac{2\mu_i}{\alpha_i^2} \left(\bar{\lambda}_1^{\alpha_i} + \bar{\lambda}_2^{\alpha_i} + \bar{\lambda}_3^{\alpha_i} - 3 \right) + \sum_{i=1}^{N} \frac{1}{D_i} (J - 1)^{2i}$$

where $\bar{\lambda}_i$ denotes the deviatoric principle stretches, J is the elastic volume strain and μ_i, α_i, and D_i are the hyperelastic constants, and i represents the order of the equation.

These constitutive equations were determined by fitting to the circumferential stress–strain data of human coronary artery as published in [10] and the tensile stress–strain hypocellular atherosclerotic plaque data published in [16].

A non-linear regression routine, available in ABAQUS, was used to obtain the constitutive models that best fit the experimental data. The stability of the material constitutive models was checked using the routine available in ABAQUS. The hyperelastic coefficients used for artery/plaque models are summarised in Table 1. The arterial components and atherosclerotic plaque were assumed to be nearly incompressible. This assumption was imposed by specifying a Poisson's ratio of 0.49, infinitesimal values for D_1, and 0 for D_2 and D_3 in the hyperelastic constitutive equations describing the materials, see Table 1.

The properties of 316L stainless steel were assigned to the stents' material. The stress–strain relationship of 316L stainless steel for Mlink$_{thin}$ (strut thickness of 50 μm) and Mlink$_{thick}$ (strut thickness of 140 μm) in the finite element models in this study were described by the mechanical

Table 1 Coefficients of the Ogden hyperelastic constitutive models

Ogden hyperelastic model constants	Intima	Media	Adventitia	Plaque
μ_1 (Pa)	−7,037,592.77	−1,231,144.96	−1,276,307.99	93,726.43
μ_2 (Pa)	4,228,836.05	785,118.59	846,408.08	–
μ_3 (Pa)	2,853,769.62	453,616.46	438,514.84	–
α_1	24.48	16.59	24.63	8.17
α_2	25.00	16.65	25.00	–
α_3	23.54	16.50	23.74	–
D_1	8.95×10^{-7}	5.31×10^{-6}	4.67×10^{-6}	4.30×10^{-7}

behaviour of the struts tested by Murphy et al. [21]. The material was described as an isotropic material with the linear elastic region of the curve defined through the bulk material values for 316L stainless steel; Young's Modulus of 196 GPa, Poisson's Ratio of 0.3. A piecewise linear function was used to represent the non-linear plasticity through a von Mises plasticity model with isotropic hardening.

2.3 Boundary conditions

The stent deployment involved expansion of the stent by the application of an internal pressure on the inner stent surface (loading), and removal of the internal pressure (unloading). A uniform, radial pressure was applied as a surface load to the internal surface of the stent increasing temporally in magnitude as a smooth step. Connector elements were utilised in ABAQUS to stop the stent from further expansion as the desired expansion diameter was achieved. These elements were connected to the centre of the stent (ground) on one end and to the stent nodes on the other end. Elements with similar function have previously been used and are outlined in detail in [5]. These connector elements simulate expansion of a stent with a non-compliant angioplasty balloon as they prevent the stent from expanding beyond the balloon diameter yet allow the characteristic *dog-boning* observed during stent expansion. The load was gradually removed to allow the stent to recoil.

Two cases were studied to compare the effect of stent strut thickness. In the first case study, both Mlink$_{thin}$ and Mlink$_{thick}$, were expanded to the initial maximum external diameter of 3.22 mm, and were allowed to recoil. In the second case study, the stents were expanded to different diameters in such a way as to achieve the same final maximum external diameter following radial recoil (3.08 mm). These values were chosen in order to expand the central stenosis in the vessel to the diameter of the proximal and distal non-atherosclerotic vessel lumen. As the diameter of the stent was found to be non-uniform in different parts of the stent following expansion, the maximum external diameter achieved by the stent was opted as a criterion for the case studies.

For both case studies the same finite element models were simulated, the only difference being the amount of pressure applied. For case study 1, 0.9 MPa (9 atm) was applied to Mlink$_{thin}$ and 1.5 MPa (15 atm) was applied to Mlink$_{thick}$, to achieve the same initial maximum external stent diameter of 3.22 mm. For case study 2, the pressure required to expand Mlink$_{thin}$ and Mlink$_{thick}$ were 1 MPa (10 atm) and 1.5 MPa (15 atm), respectively, to achieve the same final maximum external stent diameter (3.08 mm).

Cyclic symmetry boundary conditions were imposed on the nodes of the stent and artery in the circumferential plane of symmetry. The ends of the stent were free from any constraints. Displacement boundary condition was applied to both ends of the vessel to account for in situ prestretch of the vessel. Axial in situ prestretch was chosen to be 1.05 which is typical of coronary arteries. This is the upper band of the axial in situ stretch of 1.044 ± 0.06 in coronary arteries reported by Holzapfel et al. [10].

In addition, element distortion control was used to prevent incorrect results in the contact region where excessive distortion of elements could occur.

When performing a quasi-static analysis with the explicit approach it is necessary to ensure that the inertial forces are negligible and do not cause unrealistic dynamic effects. It has been shown that by maintaining the ratio of kinetic energy to the total strain energy <5% dynamic effects are negligible [13]. This criterion was adopted for the quasi-static analyses presented here.

3 Results

Radial displacements were measured at key locations on each stent through the loading and unloading process of the stents' expansion. The radial recoil throughout both structures of Mlink$_{thin}$ and Mlink$_{thick}$ was found to be highly non-uniform. The lowest values of recoil were observed at the proximal and distal ends of the stent

Table 2 Radial recoil in the stents

Stent	Pressure (atm)	Stent expanded diameter (mm)	Stent diameter following recoil (mm)	Distal end (%)	Centre (%)	Proximal end (%)
Mlink$_{thick}$	15	3.22	3.08	4.54	5	4.88
Mlink$_{thin}$	10	3.40	3.08	6.95	9.63	6.52
Mlink$_{thin}$	9	3.22	3.02	6.56	6.93	5.8

structures because of lower plaque thickness at the two ends and the radial recoil was higher for the Mlink$_{thin}$ when compared with Mlink$_{thick}$, see Table 2. Radial recoil was in the order of 3–9%, which is higher than that reported by the manufacturers for the laser cut stainless steel multilink stents (1.7–4.8%) [24, 25]. This is due to the fact that recoil is generally reported for free expansion of stents whilst the presence of the stenotic artery around the stent increased the radial recoil of the stents.
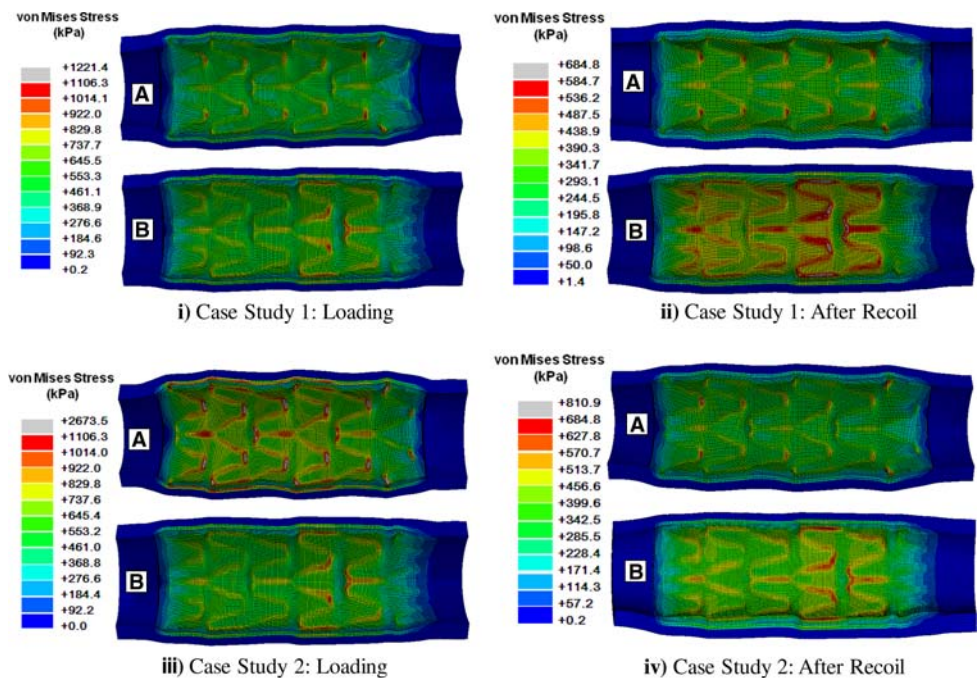
Investigating the stresses induced in the arteries by the two stents with different strut thickness it was found that the Mlink$_{thick}$ induced 15% higher stress values in the intima than the Mlink$_{thin}$ on loading to achieve the same initial maximum stent diameter, see Fig. 2. However, it was on unloading that the greatest difference in the mechanical environment of the vessels was observed. After removal of the expansion pressure the maximum external diameter of Mlink$_{thin}$ and Mlink$_{thick}$ was found to be 3.02 and 3.08 mm, respectively. As a result of the higher recoil in the Mlink$_{thin}$ 64% lower stresses were present in the intima with 17% lower stresses induced in the plaque of the vessel scaffolded by this stent, see Figs. 2 and 3. The percentage stress volume, defined as the percentage of the

tissue volume stressed over a certain threshold to the total volume of the tissue, was also calculated based on the stress value at the element integration points. Quantifying the volume of plaque and intima tissue stressed at high levels within the vessel it was found that the Mlink$_{thick}$ had higher volumes of tissue stressed at high levels particularly in the intima following recoil, see Fig. 4.
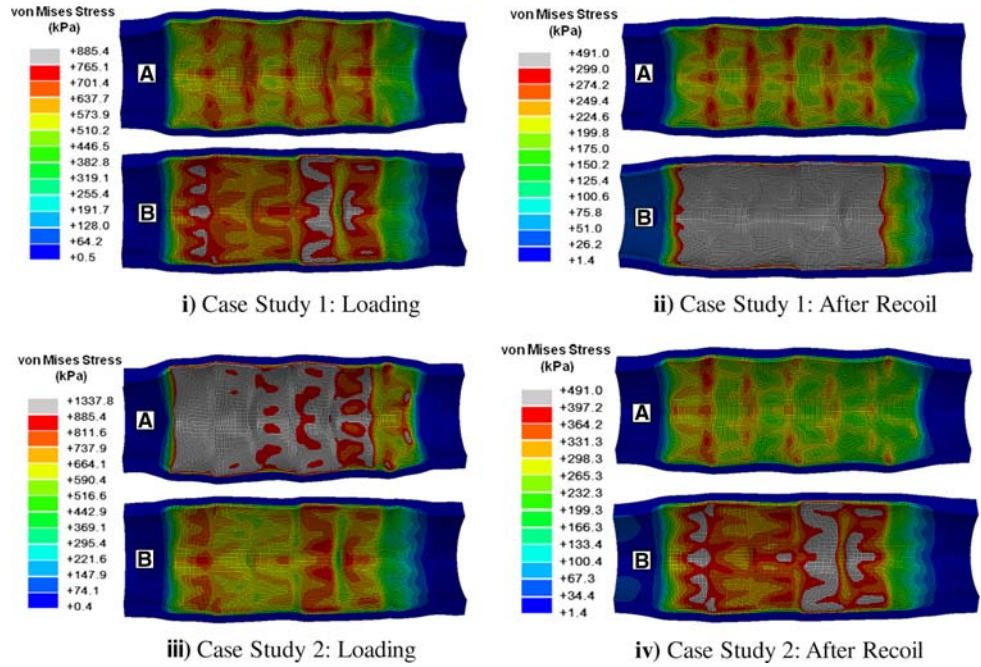
Stresses in the vessel were also investigated for case study 2, where the stents were expanded to achieve the same final maximum stent diameter. Due to the higher radial recoil observed for the Mlink$_{thin}$ it was necessary to expand it to 3.4 mm and the Mlink$_{thick}$ to 3.22 mm initial maximum external diameter to achieve a final maximum external diameter of 3.08 mm in both stented vessels.

Investigating the stresses in the vessels, it was found that due to the higher expansion diameter of the Mlink$_{thin}$ on loading it induced considerably higher stress magnitudes and volumes in the plaque tissue localised where the stent crowns contacted the plaque and intima, see Figs. 2 and 3. Removal of the lumen pressure on the stents lowered the stresses in the vessels, however, 23% higher stresses were induced in intima by Mlink$_{thick}$ following recoil, see Figs. 2, 3, 4, 5.


Fig. 2 von Mises stresses in the stenosed vessels stented with **a** multilink thin and **b** multilink thick stents

i) Case Study 1: Loading

ii) Case Study 1: After Recoil

iii) Case Study 2: Loading

iv) Case Study 2: After Recoil

Fig. 3 von Mises stresses in the intima of the stenosed vessels stented with **a** multilink thin and **b** multilink thick stents

i) Case Study 1: Loading

ii) Case Study 1: After Recoil

iii) Case Study 2: Loading

iv) Case Study 2: After Recoil

Fig. 4 The percentage stress volumes of case study one calculated for intimal tissue stressed over 300 kPa and plaque tissue stressed over 500 kPa
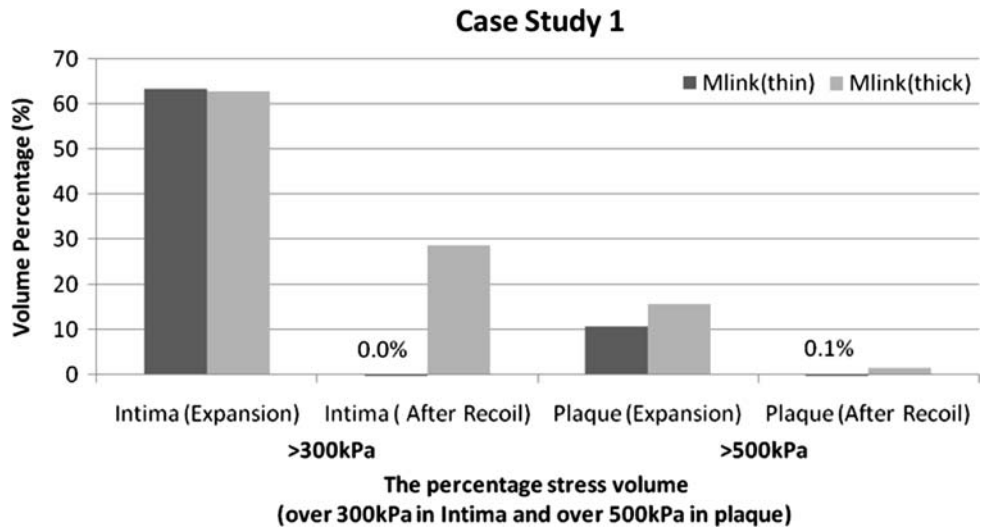
The results of these models also show that in all cases the plaque and intima of the atherosclerotic vessels undergo significantly higher stresses when compared to the media and adventitia of the vessels, see Figs. 2 and 3.

4 Discussion

The results of this study show the influence of stent strut thickness on the stresses within a vessel. If, as in the ISAR-STEREO clinical trial, two stents with the same design are expanded to the same initial maximum stent diameter the recoil of the thinner strut stent will cause lower stresses to be induced in the vessel, both acutely during the procedure,

and chronically. The stresses induced in the vessel on unloading, particularly in the intima, may act as a chronic stimulus for cell proliferation where the artery attempts to lower these stresses by vessel thickening. The lower lumen gain, but lower acute and chronic stresses, in the thinner strut stented vessel may ultimately result in less injury and aggressive healing response.

This hypothesis and the results from this numerical modelling study are supported further by the ISAR-STEREO clinical trial results whereby the diameter stenosis immediately after the procedures showed the thin-strut group had less optimal lumen gain but this was found to have significantly reversed at 6-month follow-up (see Fig. 1 in [12]).

Fig. 5 The percentage stress volumes of case study two calculated for intimal tissue stressed over 300 kPa and plaque tissue stressed over 500 kPa
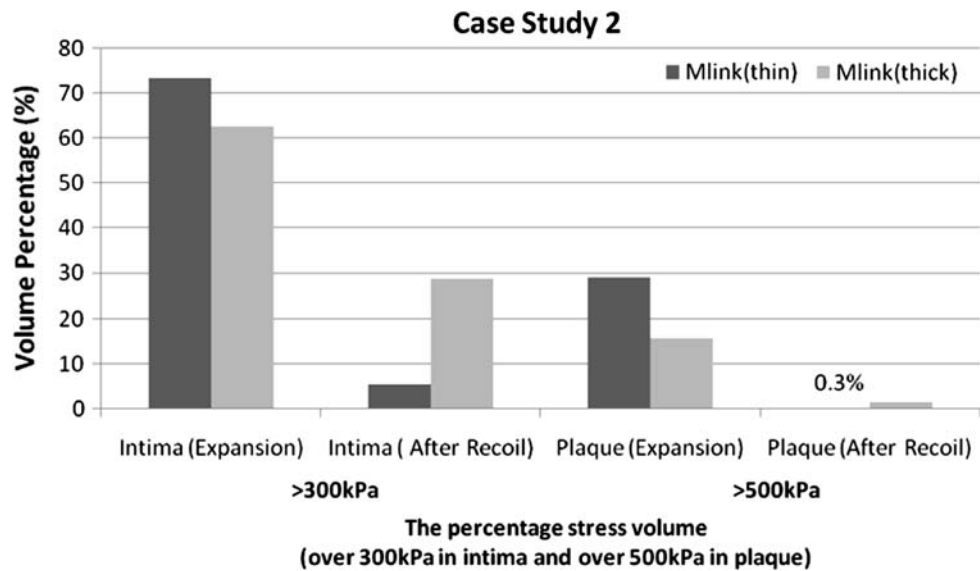
The results from case study 2 show that, although a thinner strut stent may be favourable when compared to a thicker strut stent, it only applies in cases where both stents are expanded to the same initial maximum stent diameter. Expansion of the thinner strut stent to a higher diameter to achieve the same final maximum stent diameter as the thicker strut stent results in considerably higher acute stresses at loading, however, at unloading the thicker strut stent induces 23% higher intimal stresses. Clearly therefore many stent designs, even thick-strut stents, could potentially offer a solution to restenosis if the optimum expansion diameter was considered such that stresses in the vessel were maintained low.

Manufacturers quote the recoil of stents but only for free expansion and these compare very well to those predicted using numerical models of free expansion. However, experience from our lab using commercially available stents has shown that recoil is significantly higher in stented vessels when compared to that quoted by manufacturers for free expansion [27]. This is also clearly demonstrated in the models presented here and it demonstrates the need for accurate numerical models of medical devices. In addition the numerical models show that the recoil at different locations of stents is influenced by the geometry of the stenosed vessel. The recoil in proximal and distal ends of the stent undergo lower recoil compared to the centre because of the lower thickness of the plaque at these locations.

Clearly therefore, a major concern in the response of a vessel to a stent is the stent recoil which influences the stresses induced in the vessel, however, overall stent compliance may also be a factor influencing restenosis. A more flexible, compliant stent may recoil more than a thicker strut, more rigid stent and may also therefore allow

greater conformability and scaffolding in a tortuous vessel. In addition, arterial vessels contain living cells, such as smooth muscle cells (SMCs), which are conditioned to thrive in a cyclic strain environment. Stenting lowers vessel compliance and consequently reduces the cyclic strain on these cells [29]. Altering the cyclic strain on SMCs may cause cells to proliferate as has been identified in studies on the influence of cyclic loading versus static cells in culture [19]. A thinner strut stent may stiffen a vessel to a lesser extent when compared to a thicker strut stent resulting in the cells experiencing closer to the normal cyclic strain stimulus.

The main observations from this study, however, are that a thinner strut stent induces considerably lower chronic vessel stresses when expanded to the same initial diameter as a thicker strut stent and marginally lower when expanded to the same final diameter as a thicker strut stent. Given the lower clinical restenosis rates observed for such thinner strut stents it may be postulated that there is a critical chronic stress or injury level above which intimal hyperplasia occurs which ultimately results in restenosis. It is this critical stress level that needs further investigation in clinical trials. Guidelines on this critical stress level in arteries would enable preclinical testing tools to provide better design solutions to the problem of in-stent restenosis. Future work to investigate the activity of SMCs in response to various cyclic strain levels will be carried out to determine this critical stress level.

Some limitations of this study include the use of only circumferential tensile test properties and therefore defining the arterial layers as isotropic materials, however, this assumption is plausible as the dominant mechanical properties of the arterial wall during stent deployment are the circumferential properties. Residual stresses and blood

pressure were not included in the vessels, however, given the comparative nature of this study the results are not compromised.

In addition, the tissues were assumed to be purely elastic and damage accumulation within the atherosclerotic vessel was not accounted for as it was deemed beyond the scope of this study.

Another factor which has been hypothesised to contribute to the onset of in-stent restenosis is alterations in the fluid flow within a vessel, and particularly abnormal wall shear stresses. Factors such as the separation and recirculation of the blood downstream from the stent struts have been shown to be influenced by strut spacing [4]. Although blood flow within the stented vessels has not been investigated as part of this study, it is possible that alterations in fluid flow would also vary with strut thickness and therefore influence the potential for restenotic growth within a stented vessel.

In the ISAR-STEREO trial, stent strut thickness was not strictly the only difference between the two stent designs implanted. The design of the two models is very similar except for a slightly decreased number of inter-ring articulations in the thick-strut stent (ACS Multi-Link RX DUET) when compared to the thin strut stent (ACS RX Multi-Link). The clinical study itself, however, did not consider these differences significant and therefore simply considered the study an investigation of strut thickness. In this paper we have adopted a similar approach by solely investigating the influence of the strut thickness variation and using the ACS Multi-Link RX DUET stent design only.

Clearly however, the results from the numerical models in this study demonstrate that an optimum stent design should recoil sufficiently to prevent overstressing the vessel wall whilst maintaining patency of the vessel. This study also provides evidence that preclinical testing using numerical modelling can provide insights into the optimum loading for a particular stent design to reduce the stimulus for in-stent restenosis.

References

1. Bedoya J, Meyer CA, Timmins LH, Moreno MR, Moore JE Jr (2006) Effects of stent design parameters on normal artery wall mechanics. J Biomech Eng 128:757–765
2. Briguori C, Sarais C, Pagnotta P et al (2002) In-stent restenosis in small coronary arteries: impact of strut thickness. J Am Coll Cardiol 40:403–409. doi:10.1016/S0735-1097(02)01989-7
3. de Quadros AS, Sarmento-Leite R, Gottschall CA, Silva GV, Perin EC (2006) Hyperexpansion of coronary stents and clinical outcomes. Tex Heart Inst J 33:437–444
4. Duraiswamy N, Schoephoerster RT, Moreno MR, Moore JE Jr (2007) Stented artery flow patterns and their effects on the artery

wall. Annu Rev Fluid Mech 39:357–382. doi:10.1146/annurev.fluid.39.050905.110300
5. Early M, Lally C, Prendergast PJ, Kelly DJ (2008) Stresses in peripheral arteries following stent placement: a finite element analysis. Comput Methods Biomech Biomed Engin (in press)
6. Fischman DL, Leon MB, Baim DS (1994) A randomized comparison of coronary-stent implantation with balloon angioplasty in patients with coronary artery disease. N Engl J Med 331:496–501. doi:10.1056/NEJM199408253310802
7. Grewe PH, Deneke T, Machraoui A, Barmeyer J, Muller K-M (2000) Acute and chronic tissue response to coronary stent implantation: pathologic findings in human specimens. J Am Coll Cardiol 35:157–163. doi:10.1016/S0735-1097(99)00486-6
8. Hara H, Nakamura M, Palmaz JC, Schwartz RS (2006) Role of stent design and coatings on restenosis and thrombosis. Adv Drug Deliv Rev 58:377–386. doi:10.1016/j.addr.2006.01.022
9. Holzapfel GA, Stadler M, Gasser TC (2005) Changes in the mechanical environment of stenotic arteries during interaction with stents: computational assessment of parametric stent designs. J Biomech Eng 127:166–180
10. Holzapfel GA, Sommer G, Gasser CT, Regitnig P (2005) Determination of layer-specific mechanical properties of human coronary arteries with nonatherosclerotic intimal thickening and related constitutive modeling. Am J Physiol Heart Circ Physiol 289:H2048–H2058. doi:10.1152/ajpheart.00934.2004
11. Hwang C-W, Wu D, Edelman ER (2001) Physiological transport forces govern drug distribution for stent-based delivery. Circulation 104:600–605. doi:10.1161/hc3101.092214
12. Kastrati A, Mehilli J, Dirschinger J et al (2001) intracoronary stenting and angiographic results: strut thickness effect on restenosis outcome (ISAR-STEREO) trial. Circulation 103:2816–2821
13. Kim J, Kang Y-H, Choi H-H, Hwang S-M, Kang B-S (2002) Comparison of implicit and explicit finite-element methods for the hydroforming process of an automobile lower arm. Int J Adv Manuf Technol 20:407–413. doi:10.1007/s001700200170
14. Lally C, Dolan F, Prendergast PJ (2005) Cardiovascular stent design and vessel stresses: a finite element analysis. J Biomech 38:1574–1581. doi:10.1016/j.jbiomech.2004.07.022
15. Liang DK, Yang DZ, Qi M, Wang WQ (2005) Finite element analysis of the implantation of a balloon-expandable stent in a stenosed artery. Int J Cardiol 104:314–318. doi:10.1016/j.ijcard.2004.12.033
16. Loree HM, Grodzinsky AJ, Park SY, Gibson LJ, Lee RT (1994) Static circumferential tangential modulus of human atherosclerotic tissue. J Biomech 27:195–204. doi:10.1016/0021-9290(94)90209-7
17. McClean R, Eigler NL (2002) Stent design: implications for restenosis. Rev Cardiovasc Med 3:S16–S22. doi:10.1016/S1522-1865(02)00137-3
18. Migliavacca F, Petrini L, Colombo M, Auricchio F, Pietrabissa R (2002) Mechanical behavior of coronary stents investigated through the finite element method. J Biomech 35:803–811. doi:10.1016/S0021-9290(02)00033-7
19. Morrow D, Sweeney C, Birney YA et al (2005) Cyclic strain inhibits notch receptor signaling in vascular smooth muscle cells in vitro. Circ Res 96:567–575. doi:10.1161/01.RES.0000159182.98874.43
20. Morton AC, Crossman D, Gunn J (2004) The influence of physical stent parameters upon restenosis. Pathol Biol 52:196–205. doi:10.1016/j.patbio.2004.03.013
21. Murphy BP, Savage P, McHugh PE, Quinn DF (2003) The stress–strain behaviour of coronary stent struts is size dependent. Ann Biomed Eng 31:686–691. doi:10.1114/1.1569268
22. Ogden RW (1972) Large deformation isotropic elasticity: on the correlation of theory and experiment for incompressible

rubberlike solids. Proc R Soc Lond A Math Phys Sci 326:565–584. doi:10.1098/rspa.1972.0026

23. Pache J, Kastrati A, Mehilli J et al (2003) Intracoronary stenting and angiographic results: strut thickness effect on restenosis outcome (ISAR-STEREO-2) trial. J Am Coll Cardiol 41:1283–1288. doi:10.1016/S0735-1097(03)00119-0

24. Serruys PW, Kutryk MJB (1998) Handbook of coronary stents, 2nd edn. Martin Dunitz Ltd, London

25. Serruys PW, Kutryk MJB (2000) Handbook of coronary stents, 3rd edn. Martin Dunitz Ltd, London

26. Timmins LH, Moreno MR, Meyer CA, Criscione JC, Rachev A, Moore JE Jr (2007) Stented artery biomechanics and device design optimization. Med Biol Eng Comput 45(5):505–513. doi:10.1007/s11517-007-0180-3

27. Toner D, Dolan F, Lally C (2007) Validation of numerical models of stent expansion using an in-vitro compliant artery model. In: Proceedings of bioengineering in Ireland (13) and the 27th meeting of the Northern Ireland Biomedical Engineering Society, Enniskillen, p 61

28. van Andel CJ, Pistecky PV, Borst C (2003) Mechanical properties of porcine and human arteries: implications for coronary anastomotic connectors. Ann Thorac Surg 76:58–65. doi:10.1016/S0003-4975(03)00263-7

29. Vernhet H, Demaria R, Juan JM, Oliva-Lauraire MC, Senac JP, Dauzat M (2001) Changes in wall mechanics after endovascular stenting in the rabbit aorta: comparison of three stent designs. AJR Am J Roentgenol 176:803–807